HYDROLOGICAL PROCESSES
Hydrol. Process. **15**, 825–842 (2001)
DOI: 10.1002/hyp.188

Predicting floodplain inundation: raster-based modelling versus the finite-element approach

M. S. Horritt* and P. D. Bates
School of Geographical Sciences, University of Bristol, University Road, Bristol BS8 1SS, UK

Abstract:

We compare two approaches to modelling floodplain inundation: a raster-based approach, which uses a relatively simple process representation, with channel flows being resolved separately from the floodplain using either a kinematic or diffusive wave approximation, and a finite-element hydraulic model aiming to solve the full two-dimensional shallow-water equations. A flood event on a short (*c*. 4 km) reach of the upper River Thames in the UK is simulated, the models being validated against inundation extent as determined from satellite synthetic aperture radar (SAR) imagery. The unconstrained friction parameters are found through a calibration procedure, where a measure of fit between predicted and observed shorelines is maximized. The raster and finite-element models offer similar levels of performance, both classifying approximately 84% of the model domain correctly, compared with 65% for a simple planar prediction of water surface elevation. Further discrimination between models is not possible given the errors in the validation data. The simple raster-based model is shown to have considerable advantages in terms of producing a straightforward calibration process, and being robust with respect to channel specification. Copyright © 2001 John Wiley & Sons, Ltd.

KEY WORDS flood modelling; finite elements; remote sensing; calibration

INTRODUCTION

Floodplain inundation is a major environmental hazard (see Penning-Rowsell and Tunstall, 1996) in both the developed and developing world, and in the UK, for example, the *1991 Water Resources Act* lays down a statutory requirement to provide flood extent maps for many river reaches in order to aid planning decisions and for flood warning purposes. Yet no consensus exists concerning the level of model and data complexity required to achieve a useful prediction of inundation extent, and a number of techniques present themselves for the prediction of inundation extent resulting from fluvial flood events. Although physical models and flume studies have been used to investigate complex channel flows (Thomas and Williams, 1994; Lin and Shiono, 1995; Cokljat and Kralj, 1997; Ye and McCorquodale, 1998, Bates *et al.*, 1999; Sofialidis and Prinos, 1999), numerical models offer far more flexibility in their application, and advances in numerical techniques and computing power mean that increasingly complex flows can be modelled within practical time-scales. The numerical modelling strategy required to capture important processes in floodplain inundation events is, however, still a subject of debate. There is also the question of data provision, and most modelling studies are limited by the data available, and it is obvious that it would be wasteful to use a complex process representation in a model that cannot be parameterized with sufficient accuracy. Indeed it is unclear whether time, effort and money is better spent on improving process representation in inundation models or in gathering more data for their parameterization.

One-dimensional models of channel flow, solving either the full or some approximation to the one-dimensional St Venant equations (e.g. Moussa and Bocquillon, 1996; Rutschmann and Hager, 1996), have

* Correspondence to: M. S. Horritt, School of Geographical Sciences, University of Bristol, University Road, Bristol BS8 1SS, UK. E-mail: Matt.Horritt@Bristol.ac.uk

Received 14 February 2000
Accepted 18 September 2000

long been popular for reasons of computational simplicity and ease of parameterization, but neglect important aspects of the spatially variable flood hydraulics. A two-dimensional approach is capable of resolving some hydraulic processes induced by floodplain topography and a meandering channel, which a one-dimensional model is incapable of representing. The disadvantage of two-dimensional models when compared with the one-dimensional approach is that they tend to be more data intensive, requiring distributed topographic (Bates *et al*., 1998A) and possibly friction (Horritt, 2000a) data, and distributed validation data. This has been a major argument against the use of two-dimensional models for operational inundation prediction, and these arguments apply even more strongly to three-dimensional modelling of fluvial flows.

It would seem that two-dimensional modelling is the way forward for floodplain inundation prediction for two reasons. Firstly, the process representation issues discussed above indicate that a one-dimensional model is too simplistic in its treatment of floodplain flows, and that a three-dimensional model is unnecessarily complex and computationally intensive. Secondly, techniques have been developed recently which may be used to parameterize and validate two-dimensional flood models using remote sensing data. Previously, the application of fine-scale two-dimensional hydraulic models was hampered by the scarcity of detailed topographic data, but the advent of laser altimetry and its potential for routine (and relatively inexpensive, when compared to aerial stereophotogrammetry) mapping of flood-prone areas (Ritchie, 1995, Richie *et al*., 1996, Gomes-Pereira and Wicherson, 1999) means that high resolution (*c*. 5 m), high accuracy ($\pm$20 cm) digital elevation models (DEMs) may soon be available for many rivers. Remote sensing also can provide validation data on flood extent (Bates *et al*., 1997), especially from satellite imaging radar (Horritt *et al*., 2000a) with its all weather capability. With these techniques available, we are in a position to assess the relative value of model parameterization (in terms of topography) and process representation (in terms of the increasing complexity of one-dimensional, two-dimensional finite-difference and two-dimensional finite-element models). The question of the relative importance of input data, process representation and model validation is a complex one, because these factors are interrelated. A model capturing complex hydraulic processes is essentially useless if no suitable validation data exist, or if it cannot be suitably parameterized owing to the poor quality of available topographic data. Conversely, a very high quality DEM may be wasted if its effects are lumped into the input of a very crude model.

An attempt to answer the above question is made in Bates and De Roo (2000). A raster-based model for predicting inundation extent is developed and applied to a 35-km reach of the River Meuse in The Netherlands for which a high-resolution airphotograph DEM is available. Good results are obtained using the raster model, and it is found to be an improvement over both a simple planar water-surface predictor and a finite-element model of the same reach. The study tentatively indicates that topography is more important than process representation for predicting inundation extent, and a relatively simple model can be used to good effect. There are, however, a number of issues that need to be addressed before this conclusion is substantiated. Bates and De Roo (2000) identified a number of areas for future model development and testing which are addressed in this paper. Firstly, the comparison has been carried out without calibration. Friction coefficients for the floodplain and channel are generally ill-defined, and it is usual practice to vary the values of these coefficients to obtain an optimum level of fit between model predictions and the observed flood. The fact that the two models used in Bates and De Roo, 2000, give different results despite using the same friction parameterization is unsurprising, as it is generally supposed that shortfalls in process representation can, to some extent, be compensated for by varying friction values in the calibration process. The comparative performance of the two models will be revealed only when the frictional parameter space is more fully explored. Secondly, differences may be caused by the different resolutions of the two models, the raster model at 25 m and the finite-element model with elements ranging in size between 50 m and 250 m. The disparity in scale results from pragmatic considerations: the raster model's simpler representation of floodplain hydraulic process allows it to operate at a much higher resolution than the finite-element model for given computational resources. The better performance of the raster model may be a result of this advantage of scale and hence its ability to represent small-scale processes and topography more realistically, an opportunity not available to the finite-element approach at its relatively coarse scale. Thirdly,

the raster model developed exhibits a disparity between the processes represented in the channel and on the floodplain. Channel flow is resolved using a kinematic wave approximation, whereas flows on the floodplain are predicted using an approximate diffusion-wave approach. This difference may generate spurious hydraulic features, as, for example, the kinematic wave approach allows the free surface height to increase in the flow direction (i.e. water flowing uphill), which could cause reverse flow on regions of the floodplain near the channel.

In this paper, we aim to address some of the shortcomings listed above and to validate the raster-based model of Bates and De Roo (2000) and a generalized finite-element code against flood extent (derived from satellite radar imagery) for a short reach of the River Thames, UK. The short reach length will allow both models to be tested within the constraints of current computational resources at a similar resolution, and with simulation times short enough to allow full calibration with respect to friction parameterization. Some improvements are also made to the raster model in order to include diffusion terms in the channel flow description. The aim of the research is to verify with a higher degree of certainty some of the preliminary conclusions drawn in Bates and De Roo (2000), chiefly that topography and model scale are more important in determining flood extent than the complexity of hydraulic processes represented by the model.

MODEL DESCRIPTIONS

Raster inundation model: LISFLOOD-FP

This model is described fully in Bates and De Roo (2000), but the salient points are reproduced here along with improvements made to the model subsequent to the original paper. Channel flow is handled using a one-dimensional approach that is capable of capturing the downstream propagation of a floodwave and the response of flow to free surface slope, which can be described in terms of continuity and momentum equations as

$$\frac{\partial Q}{\partial x} + \frac{\partial A}{\partial t} = q \tag{1}$$

$$S_0 - \frac{n^2 P^{4/3} Q^2}{A^{10/3}} - \left[\frac{\partial h}{\partial x}\right] = 0 \tag{2}$$

where Q is the volumetric flow rate in the channel, A the cross-sectional area of the flow, q the flow into the channel from other sources (i.e. from the floodplain or possibly tributary channels), S_0 the down-slope of the bed, n the Manning's coefficient of friction, P the wetted perimeter of the flow, and h the flow depth. In this case, the channel is assumed to be wide and shallow, so the wetted perimeter is approximated by the channel width. The term in brackets is the diffusion term, which forces the flow to respond to both the bed slope and the free surface slope, and can be switched on and off in the model, to enable both kinematic and diffusive wave approximations to be tested. With the diffusion term switched off, Equation (2) can be solved for the flow Q in terms of the cross-section A, and hence a partial differential equation in A is derived from Equation (1). Usually, Q is chosen as the dependent variable (Chow, 1988, p. 296), as it results in smaller relative errors in the estimation of discharge. For this model, however, we are interested primarily in water levels (which dictate the flood extent), so the cross-sectional area A is used as the dependent variable. It also simplifies the inclusion of the diffusion term. An explicit non-linear finite-difference system in A is then solved using the Newton–Raphson technique, rather than the linearized scheme used in the original model. The diffusion term can be included in an explicit fashion simply by modifying the bed slope, S_0, to include the depth-gradient term. This approach can cause instability and the development of saw-tooth oscillations in the solution, but these are easily countered by the use of a smaller time step. If this is the case, the time steps

for solving for channel and floodplain flows can be effectively decoupled by using a number of sub-iterations for the channel flow.

A flow rate is imposed at the upstream end of the reach, which for the kinematic wave model is sufficient as a boundary condition, as wave effects can only propagate downstream, and no backwater effects need to be taken into account. If the diffusion term is included, some downstream boundary condition is required to close the solution, as backwater effects are taken into account. This either can be a stage reading, or a zero free-surface slope condition can be imposed, which leaves the depth at the downstream boundary free to vary, but prevents the solution developing a draw-down or draw-up curve. (This option will be referred to as a free downstream boundary condition.)

The channel parameters required to run the model are its width, bed slope, depth (for linking to floodplain flows) and Manning's n value. Width and depth are assumed to be uniform along the reach, their values assuming the average values taken from channel surveys. A uniform bed slope is calculated from the DEM (which is assumed to be too coarse to contain any explicit channel information), by linear regression along the line of the channel, which is defined by a series of vectors derived from large-scale maps of the reach. It will be possible to derive such channel parameters from high-resolution DEMs automatically. The remaining friction coefficient is left as a calibration parameter.

Floodplain flows are similarly described in terms of continuity and momentum equations, discretized over a grid of square cells, and two options exist in the model for the treatment of floodplain flows. Most simply, we can assume that the flow between two cells is a function of the free surface height difference between those cells (Estrela and Quintas, 1994)

$$\frac{\mathrm{d}h^{i,j}}{\mathrm{d}t} = \frac{Q_x^{i-1,j} - Q_x^{i,j} + Q_y^{i,j-1} - Q_y^{i,j}}{\Delta x \Delta y} \tag{3}$$

$$Q_x^{i,j} = \frac{h_{\mathrm{flow}}^{5/3}}{n} \left(\frac{h^{i-1,j} - h^{i,j}}{\Delta x} \right)^{1/2} \Delta_y \tag{4}$$

where $h^{i,j}$ is the water free surface height at the node (i, j), Δx and Δy are the cell dimensions, n is the Manning's friction coefficient for the floodplain, and Q_x and Q_y describe the volumetric flow rates between floodplain cells: Q_y is defined analogously to Equation (4). The flow depth, h_{flow}, represents the depth through which water can flow between two cells, and is defined as the difference between the highest water free surface in the two cells and the highest bed elevation (this definition has been found to give sensible results for both wetting cells and for flows linking floodplain and channel cells.) The second option is to discretize the diffusive wave equation over the grid

$$Q_x^{i,j} = \frac{\dfrac{h_{\mathrm{flow}}^{5/3}}{n} \left(\dfrac{h^{i-1,j} - h^{i,j}}{\Delta x} \right) \Delta y}{\left[\left(\dfrac{h_{i-1,j} - h^{i,j}}{\Delta x} \right)^{1/2} + \left(\dfrac{h^{i,j-1} - h^{i,j+1}}{2\Delta y} \right)^{1/2} \right]^{1/4}} \tag{5}$$

This form of the flow equation can be derived from Equation (6) below (neglecting the acceleration and advection terms), solving for $|v|$ by taking the magnitude of the equation. The two approaches are subtly different: in the diffusive approach, the x, y components of the flow are linked, whereas in the cellular approach, the flow between cells is solely a function of the component of free surface gradient in that direction. A possible criticism of the cellular approach is that it fails to reproduce some (intuitively correct) features of floodplain flows. For example, flow may not be parallel to the free surface gradient, depending on the orientation of the free surface slope and the model grid, but the two approaches agree when the slope is parallel to one of the grid axes. The differences between the two models can be derived analytically for a free surface slope of unit magnitude as a function of direction. The flow vectors differ in magnitude by a mean

value of $c.$ 20% and in angle by $c.$ 10°. Although these deviations may be compensated for partially in the friction calibration process (the cellular approximation predicts larger flows than the diffusive approximation), the effect on the bulk flow behaviour of the model is unclear, and so both approximations are tested in this study. Whichever approximation is adopted, an explicit scheme is used: floodplain flows are calculated first using Equation (4 or 5), then the water depths on the floodplain are updated using Equation (3).

Equations (4 or 5) are also used to calculate flows between floodplain and channel cells, allowing floodplain cell depths to be updated using Equation (3) in response to flow from the channel. These flows are also used as the source term in Equation (1), effecting the linkage of channel and floodplain flows. Thus only mass transfer between channel and floodplain is represented in the model, and this is assumed to be dependent only on relative water-surface elevations. Although this neglects effects such as channel–floodplain momentum transfer and the effects of advection and secondary circulation on mass transfer, it is the simplest approach to the coupling problem and should reproduce some of the behaviour of the real system.

Generalized finite-element model: TELEMAC-2D

The TELEMAC-2D (Bates and Anderson, 1993, Hervouet and Van Haren, 1996) model has been applied to fluvial flooding problems for a number of river reaches and events (Bates *et al.*, 1998b). The model solves the two-dimensional shallow-water (also known as Saint-Venant or depth-averaged) equations of free surface flow

$$\frac{\partial \boldsymbol{v}}{\partial t} + (\boldsymbol{v} \cdot \nabla)\boldsymbol{v} + g\nabla(z_0 + h) + \frac{n^2 g \boldsymbol{v}|\boldsymbol{v}|}{h^{4/3}} = 0 \tag{6}$$

$$\frac{\partial h}{\partial t} + \nabla(h\boldsymbol{v}) = 0 \tag{7}$$

where $\boldsymbol{v}$ is a two-dimensional depth averaged velocity vector, h is the flow depth, z_0 the bed elevation, g the acceleration resulting from gravity, ρ the water density and n is Manning's coefficient of friction. The TELEMAC-2D model uses Galerkin's method of weighted residuals to solve Equations (6) and (7) over an unstructured mesh of triangular finite elements. A streamline-upwind-Petrov–Galerkin (SUPG) technique is used for the advection of flow depth to reduce the spurious spatial oscillations in depth that Galerkin's method is predisposed to, and the method of characteristics is used for the advection of velocity. An element-by-element solver is used to solve the non-linear system, and the time development of the solutions is dealt with using an implicit finite-difference scheme. For this study, only steady-state solutions are sought, so the time step is used as a surrogate for the development of an iterative scheme, whereby the model is 'wound-up' to a stable state. The moving boundary nature of the problem is treated with a simple wetting and drying algorithm, which eliminates spurious free surface slopes at the shoreline. It also scales the height derivative term in the continuity Equation (7) (Defina *et al.*, 1994; Bates and Hervouet, 1999), but this will not affect the steady-state solutions developed here.

MODEL TESTING

Test site and validation data

A 4-km-long reach of the upper River Thames, UK, has been selected for comparison of the two models, for a number of reasons. A 50-m resolution, 25-cm precision airphotograph DEM is available, along with ground-surveyed channel cross sections. The DEM has been modified by the inclusion of a dyke (identified in maps of the reach) that runs for 500 m along the north side of the channel at the upstream end of the reach. This was found necessary to constrain the flow in this region, and if omitted causes a gross overestimation of flood extent in the upstream part of the model. A gauging station is located at the upstream end of the reach, which can provide a boundary condition for the model. The floodplain environment is entirely agricultural, being mainly made up of meadow and rough pasture, which should make for an easier calibration problem

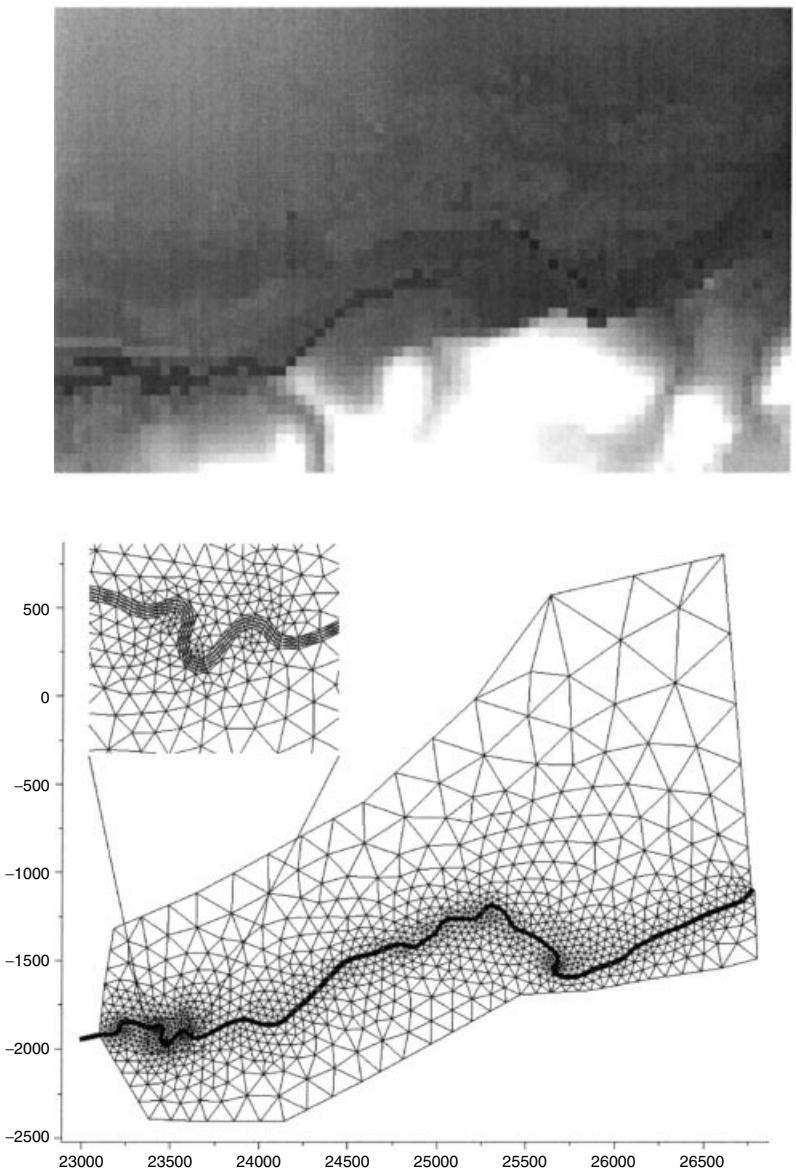

Figure 1. Finite element mesh and airphotograph topography for the Thames site

with respect to floodplain friction. Bankful discharge is estimated at 40 $m^3\ s^{-1}$, over an order of magnitude smaller than that for the reach of the Meuse (1450 $m^3\ s^{-1}$) over which the LISFLOOD-FP model has already been tested, and therefore should test the down-scaling properties of the finite-difference model. A finite-element mesh for the TELEMAC-2D model has been constructed using a streamline curvature-dependent mesh generator (Horritt, 2000b) that ensures depth prediction errors are independent of channel sinuosity. Element sizes vary from <50 m near the channel to *c*. 100 m in the shoreline region. The mesh, along with the topography and channel for the LISFLOOD-FP model, is shown in Figure 1. Steady flow is assumed throughout this study (peak inflow of 73 $m^3\ s^{-1}$), as given the short length of the reach and a typical kinematic wave propagation velocity (1·5 m s^{-1}) we would expect the reach to respond to changes in inflow in <1 h.

Even taking into account propagation times for the wetting front (measured at *c*. 3 h), this is still far quicker than significant changes in inflow (the hydrograph peak is *c*. 40 h in duration).

Validation data are also available in the form of satellite imagery (from the ERS-1 SAR sensor) of a 1-in-5 year flood event on the reach. This has been processed using a statistical active contour technique (Horritt, 1999; Horritt *et al*., in press) to extract the flood shoreline, which then also can be used to form a raster map of the inundation state. This technique has been found to delineate the shoreline with a mean location error of *c*. 50 m (Horritt *et al*., in press) when compared with airphotograph data, which is probably adequate for this study, as it is commensurate with the DEM resolution.

Model testing

Friction coefficients for the channel and floodplain remain unconstrained for this problem, and therefore are treated as calibration coefficients (Bates *et al*., 1998b; Horritt, 2000a). Although this is likely to be a major source of model error, and will certainly cloud the issue of model comparison, the lack of alternative techniques for parameterizing friction means that calibration is currently the only way forward. It also offers the opportunity of exploring the effects of friction parameterization on the modelling strategies.

Firstly, we define the extent and dimensionality of the parameter space for the calibration problem. We assume only two friction classes, one for the channel and one for the floodplain, giving a two-dimensional problem. Manning's n values for the channel range from 0·01 to 0·05, equivalent to values quoted for concrete-lined straight channels and winding natural channels with vegetation and pools, respectively (Chow, 1988, p. 35). Values for the floodplain range from 0·02 to 0·10 or 0·12 (depending on the model used, see discussion below), equivalent to a surface somewhat smoother than pasture ($n = 0{\cdot}035$) to dense trees. This enables the full range of possible frictional values to be explored. For this reach (winding channel surrounded mainly by pasture with hedgerows), we would expect the optimum calibration to occur approximately in the centre of the parameter space, but as the friction calibration is also partly used to compensate for poorly represented processes in the model, the optimum may be shifted. Exploring the entire parameter space is a computationally intensive process, so a more pragmatic approach is adopted, instead aiming to explore only sparsely the full space, but focusing more attention on the area in the region of the optimum calibration.

Before calibration can be performed, we first also need to define some measure of fit between the observed and predicted flood extent, as it is this measure that will be optimized by the calibration process. We use an area-based measure, the area correctly predicted as either wet or dry by the model, which is corrected for bias that may be introduced by the area occupied by the flood. For example, for a small flood in a large, mostly dry domain, even a relatively poor prediction of flood extent may give apparently good results in terms of the area correctly predicted by the model (i.e. the large dry area). This can be rectified by ignoring an appropriate portion of the dry area, to make it equal in size to the flood. In this case, only 15·1% of the domain is flooded and 84·9% is dry, and so in the calculation of correct area, 69·8% (84·9–15·1%) is disregarded when the model predictions and satellite data are compared, in order to give approximately equal flooded/unflooded areas.

Comparing results from the two models and the satellite data presents a little difficulty, owing to the different scales and representations of the depth field used in the models. In this case, the results from the raster model are sampled on to a 12·5 m grid (the resolution of the satellite data), and then can be compared directly on a pixel by pixel basis. The finite-element results are also sampled on to a 12·5 m grid, the depth field being linearly interpolated across each element. The treatment of shoreline regions requires special care: the water surface is extrapolated horizontally from the wet node(s) of a partially wet element and the shoreline defined as the intersection of the surface with the planar element topography. This means that the shoreline can lie within an element, rather than being confined to lying along element boundaries, which would be the case if the water surface was interpolated normally between wet and dry nodes.

The results of calibration for the LISFLOOD-FP model, using the kinematic wave approximation for channel flows and the cellular approximation over the floodplain, are summarized in Table I. The optimum

Table I. Calibration for LISFLOOD-FP model using the kinematic wave approximation for channel flow, showing fit with SAR data (% correct, corrected to remove bias) against floodplain friction (n_{fl}) and channel friction (n_{ch})

n_{ch}	n_{fl}				
	0·02	0·04	0·06	0·08	0·10
0·01	65·2		65·8		65·8
0·02		78·5	80·1	80·3	
0·03	80·9	83·3	83·8	83·6	81·9
0·04		79·9	78·3	72·1	
0·05	79·0		65·5		45·1

calibration is (by chance) in the centre of the parameter space, occurring at friction values we would expect for this channel and floodplain environment. The model also shows more sensitivity to channel friction than floodplain friction, the measure of fit being >80% for all values of floodplain friction when Manning's n for the channel is set at 0·03. The results of the calibration are also shown in Figure 2 as a contour plot of measure of fit over the parameter space, showing the optimum as a broad peak, and that the model has given a well behaved calibration problem. The best-fit solution is shown in Figure 3 with the SAR derived shoreline, showing that the model has predicted the inundation extent reasonably.

Refinements in the model process representation may improve the results. Firstly, the diffusive approximation to floodplain flow is used, and the results displayed in Figure 4. The results show now overall improvement in prediction accuracy (a maximum of c. 80%), the model is slightly more sensitive to floodplain friction than before, and the optimum friction value has been shifted. Secondly, a diffusive wave approximation may be

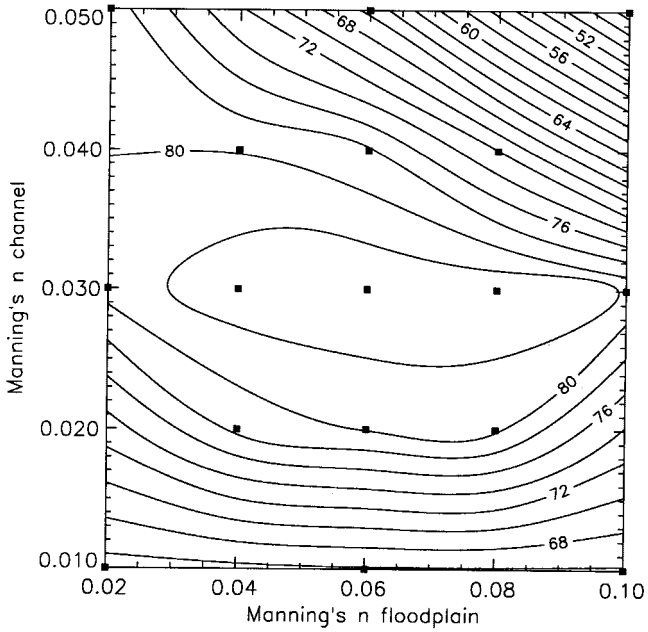

Figure 2. Results of calibration of the LISFLOOD-FP model using the kinematic wave approximation. The black squares correspond to points in the parameter space for which simulations were performed, the surface between points is found from inverse-square distance interpolation, and contoured using PV-Wave software. The contours are not meant to represent a realistic interpolation, but are merely a visualization tool

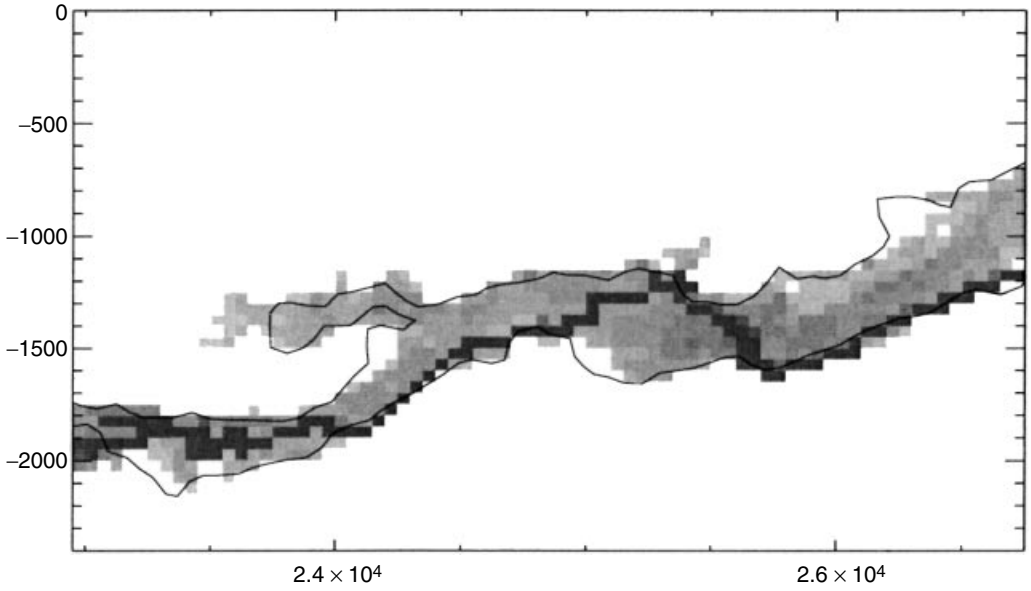

Figure 3. Best-fit solution from the LISFLOOD-FP model using the kinematic wave approximation in the channel and the cellular model for floodplain flow

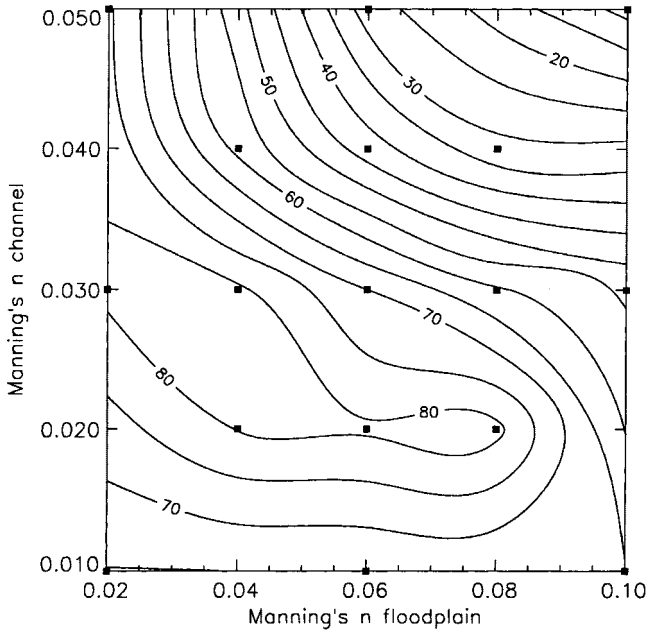

Figure 4. Results of calibration of the LISFLOOD-FP model using the kinematic wave approximation in the channel and the diffusive model for floodplain flow

used in the channel. Figure 5 shows the water surface profiles for two simulations using the kinematic and diffusive wave approximations, the kinematic model has predicted physically unrealistic variations in the free surface (induced by the linkage with floodplain flows), which are eliminated in the much smoother solution to the diffusive approximation. Nevertheless, both solutions have the same overall form, but with the diffusive

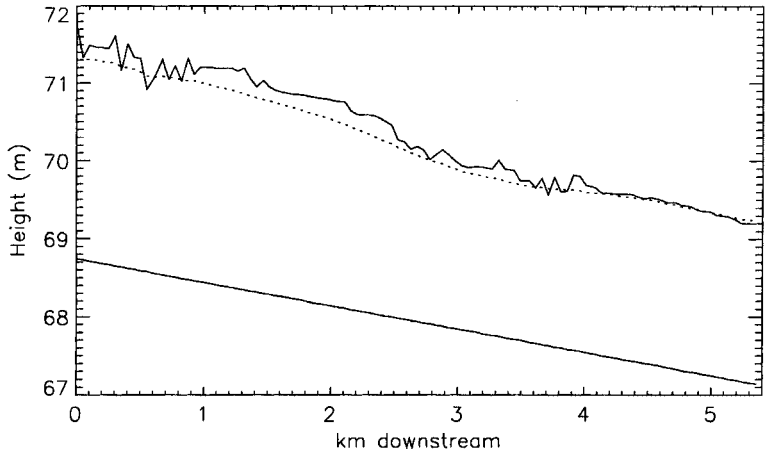

Figure 5. Water surface profiles along channel for kinematic (solid line) and diffusive (dotted line) wave models

Table II. Calibration for LISFLOOD-FP model using the diffusive wave approximation, showing fit with SAR data (% correct, corrected to remove bias) against floodplain friction (n_{fl}) and channel friction (n_{ch})

n_{ch}	n_{fl}				
	0·02	0·04	0·06	0·08	0·10
0·01	66·2				
0·02		74·2		76·1	77·2
0·03			83·5	84·2	84·0
0·04			84·7	84·7	83·7
0·05		83·2	82·7	81·3	79·7

approximation reducing water levels over the upstream half of the reach. A calibration of the diffusive channel flow scheme is given in Table II and the resulting surface shown in Figure 6. Figure 7 shows the best-fit solution for the diffusive scheme. Although the diffusive scheme has produced more realistic predictions of water depth over the channel, no overall improvement in model fit is made.

The results of the calibration of the TELEMAC-2D model are given in Table III and shown in Figure 8. The model fit covers a smaller range than for LISFLOOD, and the fit surface has a more complex form, although the higher sensitivity to channel friction is still present. The optimum fit is similar to that produced by the raster model using the kinematic wave approximation. The best TELEMAC-2D solution is shown in Figure 9 with the SAR shoreline.

The raster model seems to be capable of predicting inundation extent reasonably well, despite the rather crude assumptions of uniform bed slope, width, channel depth and friction. Refinements in the channel and floodplain flow representation have yielded no improvement in model results. It is interesting to note that the optimum channel friction gives a bankful discharge of 36 m^3 s^{-1}, close to the Environment Agency estimate of 40 m^3 s^{-1}. Table IV explores the model sensitivity to channel specification, showing that it is still possible to achieve good results from the model even using the incorrect channel parameters, as long as the bankful discharge is approximately correct. This may be indicative of a certain insensitivity of model results to channel parameters, as long as the correct volume of water is being routed over the floodplain. However, it is unlikely that this result will hold for other reaches and other (possibly dynamic) events, and may be simply a peculiarity of this particular model and data set.

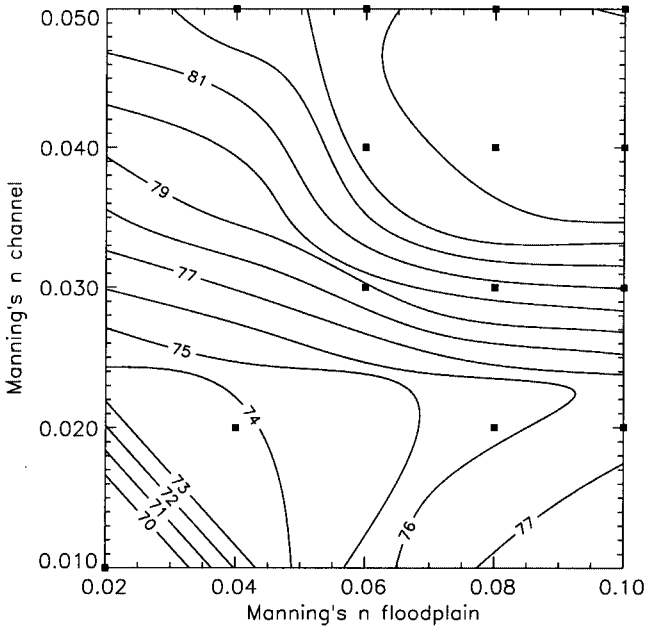

Figure 6. Calibration surface for the LISFLOOD-FP model using the diffusive wave approximation in the channel and the cellular model over the floodplain

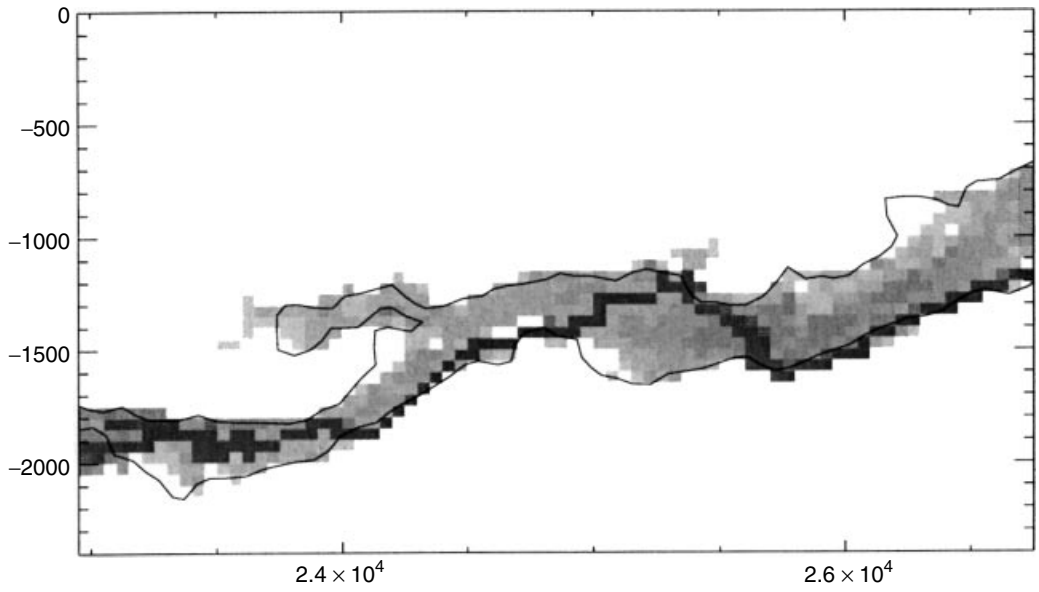

Figure 7. Best-fit solution from the LISFLOOD-FP model using the diffusive wave approximation

The numerical performance of the kinematic and diffusive raster models and the finite-element scheme also can be compared in terms of mass balance errors and computational efficiency, given in Table V. Mass balance errors are calculated over each time step as

$$Q_{\text{error}} = Q_{\text{in}} - Q_{\text{out}} - \frac{V_t - V_{t-1}}{\Delta t} \tag{8}$$

Table III. Calibration for TELEMAC-2D, showing fit with SAR data (% correct, corrected to remove bias) against floodplain friction (n_{fl}) and channel friction (n_{ch})

n_{ch}	n_{fl}					
	0·02	0·04	0·06	0·08	0·10	0·12
0·01	75·5					
0·02		79·0			79·7	
0·03			79·8	80·2	81·2	81·4
0·04			82·6	82·9	83·5	81·8
0·05		82·4	82·3	82·4	82·6	
0·06						82·0

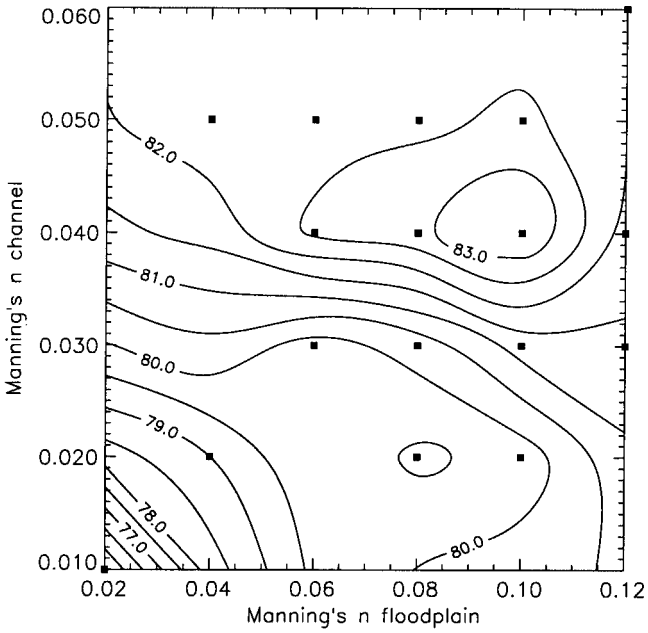

Figure 8. Calibration surface for the TELEMAC-2D model

where Q_{in} is the imposed upstream flowrate, Q_{out} is the model downstream flowrate, V_t and V_{t-1} are the volumes of water in the model domain at the current and previous time step and Δt is the model time step. The error can be thought of in terms of the volume lost or gained per second by the models. Although it is difficult to produce objective criteria of what constitute adequate mass conservation properties, the error figures given in Table V are all probably less than the error in the inflow figure used to provide the upstream boundary condition. Given that the continuity equation is also liable to process representation errors (it neglects infiltration, runoff from bounding slopes, rainfall and evaporation), the mass balance errors found here probably have an insignificant effect on the predicted inundation extent. The time taken for 1000 iterations, along with numerical parameters for the models, are also given. The diffusive raster model required a 0·5 s time step and 10 subiterations for channel flows to achieve stability, compared with 1·0 s and no extra channel subiterations for the kinematic scheme. The small time step used is a result of instabilities caused mainly by the linkage of channel and floodplain flows, the reduction of the time step and the use of subiterations being the easiest way around this problem without reformulation of the explicit model. The raster models were coded in C++

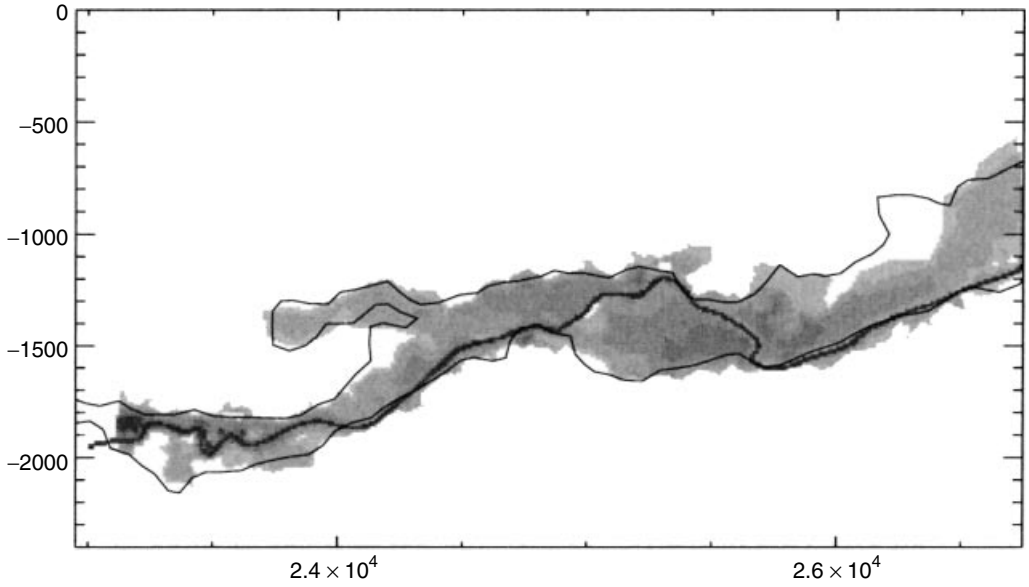

Figure 9. Best-fit solution from the TELEMAC-2D model

Table IV. LISFLOOD-FP model sensitivity to channel specification

n_{ch}	Width (m)	Depth (m)	Bankful discharge (m^3 s^{-1})	Fit (%)
0·03	10	3·03	36·6	81·3
0·03	20	2·00	36·6	83·8
0·03	30	1·57	36·6	83·6
0·03	40	1·32	36·6	83·5
0·03	80	0·87	36·6	83·1
0·02	20	1·57	36·6	84·2
0·04	20	2·00	27·4	78·3
0·02	20	2·00	54·9	80·1

Table V. Computational performance and mass balance errors for the three models

Model	Time step (s)	Subiterations	Time per 1000 iterations (s)	Absolute mass balance error (m^3 s^{-1})
LISFLOOD-FP kinematic	1·0	1	12·8	0·05
LISFLOOD-FP diffusive	0·5	10	24·4	0·03
TELEMAC-2D	2·0	—	169	0·02

and run on a 400 Mhz Pentium II processor, and TELEMAC-2D in FORTRAN on a MIPS RISC 12000 300 MHz processor in a Silicon Graphics Octane workstation. The figures show that the raster models have a considerable speed advantage over the finite-element scheme, and all the models exhibit similar mass balance errors. Given the size of the domain (76 × 48 cell), the speed of the kinematic raster model is $3{\cdot}5 \times 10^{-6}$ s per cell per time step, 50 times faster than the PC-Raster coded model used in Bates and De Roo (2000), with a speed of $1{\cdot}7 \times 10^{-4}$ s per cell per time step.

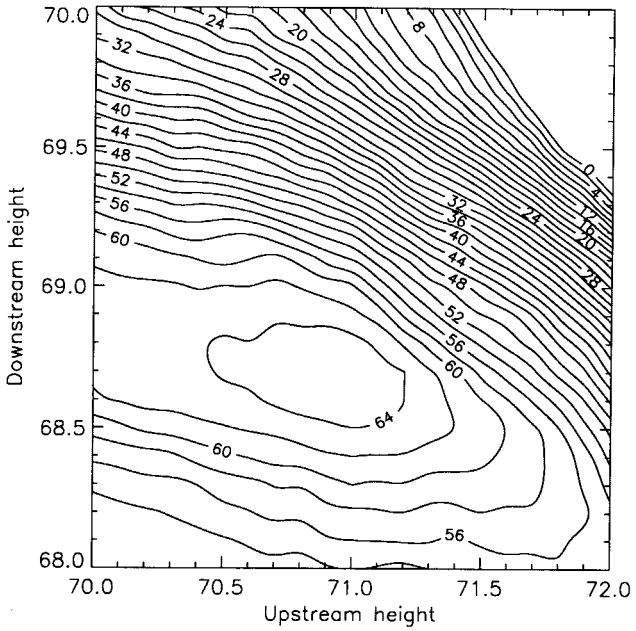

Figure 10. Calibration of planar free-surface approximation, showing measure of fit as a function of upstream and downstream water elevations

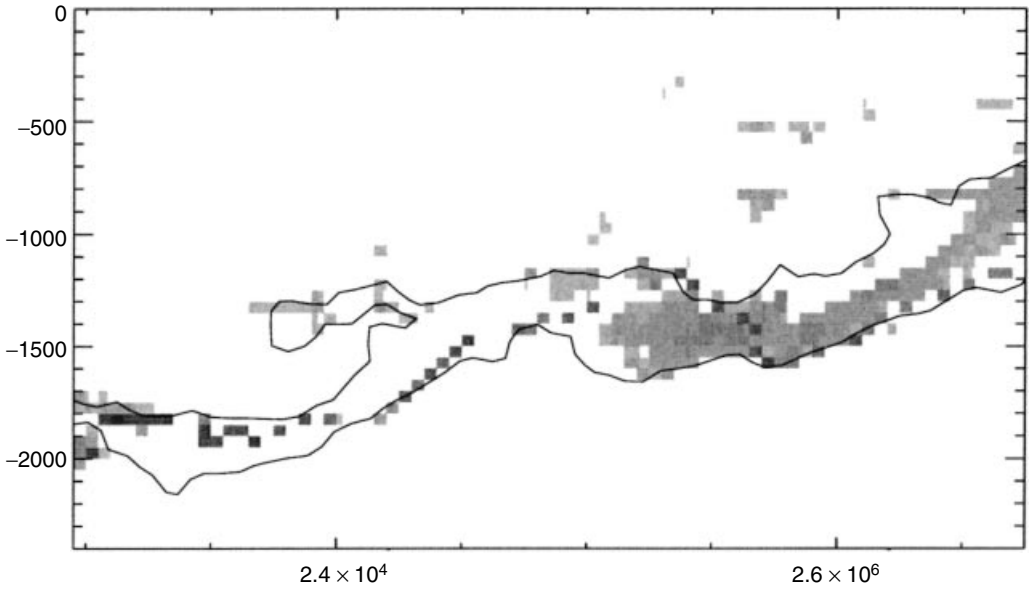

Figure 11. Best-fit solution using the planar free-surface approximation

As a final test of the performance of both models, it is useful to compare their results with those from a crude predictor of flood extent, such as a planar water free-surface height intersected with the DEM. This is a useful safeguard against the assumption that the hydraulic models are performing well, when, in fact, the problem of flood extent prediction may be trivial. The planar surface must be parameterized in terms of the heights at the upstream and downstream ends, and several techniques present themselves. The heights

can be taken from water elevations in the channel, as measured at gauging stations, or from water elevations taken from the intersection between the SAR shoreline and the DEM. Both of these techniques may be prone to error caused by small local variations in water elevation in response to local hydraulic conditions, so a calibration method was adopted instead, whereby the upstream and downstream elevations of the planar surface are adjusted and the optimum fit with the SAR data sought. The results are given in Figure 10, which shows a definite maximum (65%), and this best fit is shown in Figure 11. The calibration surface for the planar predictor shows a greater sensitivity to downstream height as the flow is less constrained at the downstream end owing to the lower transverse floodplain gradients. Given that using the unbiased measure of fit for classifying the whole of the floodplain as dry is 50%, the results of the hydraulic models (both raster and finite-element) are a significant improvement over the planar free-surface predictor. This is to be expected from the water surface profiles of Figure 5, which show a considerable curvature in the surface, which therefore will be only poorly represented by a linear approximation.

DISCUSSION

Both the raster model and the finite-element scheme have performed reasonably when compared with the satellite imagery, but it is unclear whether further progress can be made at this stage. Errors in the SAR-derived shoreline are of the order of 50 m, according to Horritt *et al*., in press, who compared SAR-derived flood shorelines against airphotograph data over two 15-km reaches of the River Thames. If this error is reproduced all along the shoreline, it is equivalent to misclassifying *c*. 4% of the domain. This equates to an unbiased measure of fit of 87%, only slightly higher than the measures of fit we are obtaining with the inundation models tested here. This implies that we are achieving a similar measure of fit between model and SAR data as between SAR data and the real flood shoreline, and any further improvement in model performance is not possible with this data set. Both the raster and the finite-element models achieve a similar measure of fit, but to distinguish further between them requires more precise validation data. This point is illustrated further in Figure 12, which shows three of the best-fit shorelines over the SAR shoreline, but

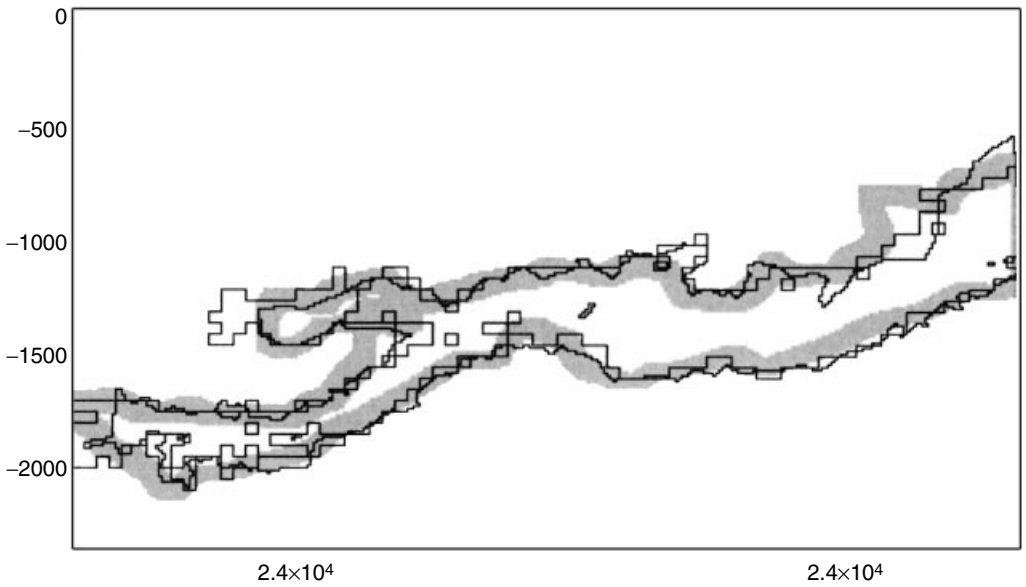

Figure 12. Shorelines for three best-fit simulations (finite element, kinematic channel/cellular floodplain and kinematic channel/diffusive floodplain) shown over the blurred SAR shoreline (in grey)

widened to represent the likely error (±50 m). In most regions the model shorelines are all within the error bounds of the validation data, and so cannot be distinguished. Some regions are more sensitive to model formulation than others (the back flooded region to the top left, for example), and in these parts one model may well be superior to another, while the overall measure of fit is still similar. It must be remembered that the optimum model formulation and calibration is not only dependent on the validation data, but the objective function used in the comparison with model predictions. The results of inappropriate process representation have thus been masked by uncertainty in the validation data, and at this level of uncertainty, a relatively crude representation is enough to reproduce the observed inundation extent.

It should be stressed that this research has focused on the use of hydraulic models as inundation predictors, and they have been tested as such against the SAR-derived shoreline data. There will be only a weak link between inundation extent and floodplain and channel hydraulics, so this research only partially validates the hydraulic representations used in the model. This is demonstrated particularly well by the raster model's robustness with respect to channel specification. Very different channel widths and depths, with the constraint that they should approximately reproduce bankful discharge, can produce similar inundation patterns and measures of fit when compared with the SAR data, but with very different hydraulic conditions operating in the channel. This property is also demonstrated by the similarity of the raster models' predictions of flood extent using the kinematic and diffusive wave approximation. The unphysical variations in the free surface over the channel predicted by the kinematic model are not reflected in the flood shoreline, perhaps because these variations are in some sense damped out in the far flow field near the shoreline. This is encouraging in terms of inundation prediction, as it appears that in this case, as long as bankful discharge is approximately correct, the inundated area also will be approximately correct. Looking at the inverse problem, however, we see that inundation extent may give us very little information about channel flows.

This study has been limited to a single test site, and further applications to different sites are required to verify or disprove the results obtained here. It is encouraging, however, that the model has now been applied to two test sites at very different scales and discharges (73 $m^3\ s^{-1}$ for the Thames site and 2800 $m^3\ s^{-1}$ for the Meuse) with similar success. There are a number of factors that may affect prediction accuracy when these modelling strategies are extended to other reaches. Inundation extent is very sensitive to topography, so the details of floodplain topography will affect the sensitivity to model formulation and calibration. Dynamic effects also may become important, especially over longer reaches. The kinematic wave velocity for the channel used here will be approximately 1·5 m s^{-1} (Chow, 1988, p. 284), and the surface wave celerity approximately 4·5 m s^{-1}, so kinematic effects should propagate along the 4 km reach in *c*. 1 h. The maximum rate of change of the hydrograph for this event is 1·3 $m^3\ s^{-1}\ h^{-1}$, so dynamic effects are unlikely to be important for this reach. Longer reaches will respond more slowly and with more complexity to the dynamic behaviour of the input hydrograph, and this may become a useful diagnostic tool for assessing model performance. For example, we have seen how the raster-based model is fairly robust with respect to channel specification, as long as bankful discharge is reproduced reasonably well. Varying channel depth does, however, also affect kinematic and diffusive wave velocities, and so changing the channel properties may have much more of an effect for dynamic simulations than the steady-state solutions developed here.

The application of hydraulic models to inundation prediction is still reliant on the calibration process, which tends to obscure model validation issues. The calibration process is model dependent: the TELEMAC-2D model produces the most complex calibration surface, whereas that for the LISFLOOD-FP model with kinematic approximation for channel flows is relatively simple, with the diffusive model somewhere in between. With all the models giving roughly the same level of fit at the optimum calibration (the optimum being model dependent), this is a point in favour of the simpler model. Given that currently we can only achieve closure in terms of friction parameterization through a calibration procedure, the simpler calibration properties of the raster model are a definite advantage.

CONCLUSIONS

All the models tested here (raster kinematic, raster diffusive and finite element) have performed to a similar level of accuracy, classifying approximately 84% of the model domain correctly when compared with SAR-derived shoreline data. However, the validation data used here are insufficiently accurate to distinguish between the model formulations, and the issue of model validation is further clouded by the calibration process necessary, owing to the lack of friction parameterization data. The remotely sensed data has proved invaluable, however, in the calibration process, and has reduced the equifinality problem inherent in calibrating distributed models with point hydrometric data. Given the likely accuracy of the validation data, and the increasing complexity of the calibration process for models representing more complex processes, the simple raster-based model using a kinematic wave approximation over the channel is the simplest (and fastest) model to use and adequate for inundation prediction over this reach.

The priorities for future research are clearly defined. Further progress in terms of model validation will be made possible with more accurate validation data, possibly from different satellite-borne or airborne sensors. The technique of model validation using remote sensing data should be applied to other reaches and events as the appropriate data sets become available. This will increase confidence in model predictions, and the study of dynamic flood events may facilitate the discrimination between different model formulations and process representations. Further progress will be possible when the need for calibration is removed, and the development of a physically based friction model would be advantageous, perhaps again using remotely sensed data, such as laser altimetry (e.g. Menenti and Ritchie, 1994).

ACKNOWLEDGEMENTS

This research has been funded by the UK Natural Environment Research Council grant GR3 CO/030. Thanks go to the (anonymous) reviewers for many helpful suggestions, and to Professor John Hogan, Department of Engineering Mathematics, University of Bristol, for an invaluable discussion on the model numerics.

REFERENCES

Bates PD, Anderson MG. 1993. A two dimensional finite element model for river flood inundation. *Proceedings of the Royal Society of London* **440**: 481–491.

Bates PD, De Roo APJ. In press. A simple raster based model for flood inundation simulation. *Journal of Hydrology* **236**: 54–77.

Bates PD, Hervouet J-M. 1999. A new method for moving-boundary hydrodynamic problems in shallow water. *Proceedings of the Royal Society of London* **455**: 3107–3128.

Bates PD, Horrit MS, Smith CN, Mason DC. 1997. Integrating remote sensing observations of flood hydrology and hydraulic modelling. *Hydrological Processes* **11**: 1777–1795.

Bates PD, Horritt MS, Hervouet J-M. 1998a. Investigating two-dimensional, finite element predictions of floodplain inundation using fractal generated topography. *Hydrological Processes* **12**: 1257–1277.

Bates PD, Stewart MD, Siggers GB, Smith CN, Hervouet J-M, Sellin RJH. 1998b. Internal and external validation of a two-dimensional finite element code for river flood simulations. *Proceedings of the Institute of Civil Engineers, Water, Maritime and Energy* **130**: 127–141.

Bates PD, Wilson CAME, Hervouet J-M, Stewart MD. 1999. Two dimensional finite element modelling of floodplain flow. *La Houille Blanche* **3/4**: 82–88.

Chow VT. 1988. *Applied Hydrology*. McGraw-Hill: New York; 572. pp.

Cokljat D, Kralj C. 1997. On choice of turbulence model for prediction of flows over river bed forms. *Journal of Hydraulics Research* **35**(3): 355–361.

Defina A, D'Alpos L, Matticchio B. 1994. A new set of equations for very shallow water and partially dry areas suitable to 2D numerical models. In *Modelling flood Propagation over Initially Dry Areas*, Molinaro P, Natale L (eds). American Society of Civil Engineers: New York; 72–81.

Estrela T, Quintas L. 1994. Use of GIS in the modelling of flows on floodplains. In *2nd International Conference on River Flood Hydraulics*, White HR, Watts J (eds). Wiley: Chichester; 177–189.

Gee DM, Anderson MG, Baird L. 1990. Large scale floodplain modelling. *Earth Surface Processes and Landforms* **15**: 512–523.

Gomes-Pereira LM, Wicherson RJ. 1999. Suitability of laser data for deriving geographical data: a case study in the context of management of fluvial zones. *Photogrammetry and Remote Sensing* **54**: 105–114.

Hervouet J-M, Van Haren L. 1996. Recent advances in numerical methods for fluid flows. In *Floodplain Processes*, Anderson MG, Walling DE, Bates PD (eds). Wiley: Chichester; 183–214.

Horritt MS. 1999. A statistical active contour model for SAR image segmentation. *Image and Vision Computing* **17**: 213–224.
Horritt MS. 2000a. Calibration and validation of a 2-dimensional finite element flood flow model using satellite radar imagery. *Water Resources Research* **36**(11): 3279–3291.
Horritt MS. 2000b. Development of physically based meshes for two-dimensional models of meandering channel flow. *International Journal for Numerical Methods in Engineering* **47**: 2019–2037.
Horritt MS, Mason DC, Luckman AJ. In press. Flood boundary delineation from synthetic aperture radar imagery using a statistical active contour technique. *International Journal of Remote Sensing*.
Lin B, Shiono K. 1995. Numerical modelling of solute transport in compound channel flows. *Journal Hydraulic Research* **33**(6): 773–787.
Menenti M, Ritchie JC. 1994. Estimation of effective aerodynamic roughness of Walnut Gulch watershed with laser altimeter measurements. *Water Resources Research* **30**(5): 1329–1337.
Moussa R, Bocquillon C. 1996. Criteria for the choice of flood-routing methods in natural channels. *Journal of Hydrology* **186**: 1–30.
Penning-Rowsell EC, Tunstall SM. 1996. Risks and resources: defining and managing the floodplain. In *Floodplain Processes*, Anderson MG, Walling DE, Bates PD (eds). Wiley: Chichester; 493–533.
Ritchie JC. 1995. Airborne laser altimeter measurements of landscape topography. *Remote Sensing of the Environment* **53**: 91–96.
Ritchie JC, Menenti M, Weltz MA. 1996. Measurements of land surface features using an airborne laser altimeter: the HAPEX–Sahel experiment. *International Journal of Remote Sensing* **17**(18): 3705–3724.
Rutschmann P, Hager W. 1996. Diffusion of floodwaves. *Journal of Hydrology* **178**: 19–32.
Sofialidis D, Prinos P. 1999. Numerical study of momentum exchange in compound open channel flow. *Journal of Hydraulic Engineering* **125**(2): 152–165.
Thomas TG, Williams JJR. 1994. Large eddy simulation of turbulent flow in an asymmetric compound channel. *Journal of Hydraulic Research* **33**(1): 27–41.
Ye J, McCorquodale JA. 1998. Simulation of curved open channel flow by 3D hydrodynamic model. *Journal of Hydraulic Engineering* **124**(7): 687–698.

